PHYSICAL REVIEW D **86,** 105016 (2012)

Functional renormalization for chiral and $U_A(1)$ symmetries at finite temperature

Yin Jiang and Pengfei Zhuang

Physics Department, Tsinghua University, Beijing 100084, China

(Received 2 September 2012; published 8 November 2012)

We investigated chiral symmetry and $U_A(1)$ anomaly at finite temperature by applying the functional renormalization group to the $SU(3)$ linear sigma model. Expanding the local potential around the classical fields, we derived the flow equations for the renormalization parameters. In the chiral limit, the flow equation for the chiral condensate is decoupled from the others and can be analytically solved. The Goldstone theorem is guaranteed in vacuum and at finite temperature, and the two phase transitions for the chiral and $U_A(1)$ symmetry restoration happen at the same critical temperature. In the general case with explicit chiral symmetry breaking, the two symmetries are partially and slowly restored, and the scalar and pseudoscalar meson masses are controlled by the restoration in the limit of high temperature.

DOI: 10.1103/PhysRevD.86.105016 PACS numbers: 11.30.Rd, 11.10.Wx

I. INTRODUCTION

Chiral symmetry is one of the fundamental properties of quantum chromodynamics (QCD). In the chiral limit with zero current quark mass, the QCD Lagrangian density respects the symmetry of $U_L(3) \times U_R(3) = U_V(1) \times U_A(1) \times SU_V(3) \times SU_A(3)$ at classical level. In vacuum, the condensate of right-handed quark and left-handed antiquark $\langle \bar{q}_L q_R \rangle$ breaks the $SU_A(3)$ symmetry, and the $U_A(1)$ is broken by the anomaly due to the nontrivial topology of the principal bundle of gauge field [1,2]. Chiral symmetry breaking leads to a rich meson and baryon spectrum, and as a supplement the $U_A(1)$ anomaly explains the nondegeneracy of η and η' mesons [3–5]. As a strong interacting system should approach its classic limit at high temperature, chiral symmetry is believed to be restored in hot medium. The relation between the two symmetries in vacuum and at finite temperature has been studied for a long time [6–8]. While the two symmetries are expected to be restored [9] at high temperature, it is still an open question whether the two phase transitions happen under the same condition.

The lattice simulation is a powerful tool to study the QCD symmetries in vacuum and at finite temperature. The chiral condensate is observed to decrease with increasing temperature, and the chiral susceptibility shows a peak at a critical temperature T_c. By a proper definition, the topological charge and its susceptibility are used to describe the $U_A(1)$ anomaly in the pure gauge field theory and the unquenched theory [10,11]. In both cases, the susceptibility drops down above the critical temperature T_c of the chiral restoration, and the charge keeps an obvious deviation from zero at high temperature $T > T_c$. The simulation for the instanton model shows such a partial restoration, too [12]. On the other hand, the observation of the hadron spectra provides an experimental way to test the restoration of the two symmetries in hot medium created in relativistic heavy ion collisions [13–15]. The mass shift due to the chiral restoration enhances or reduces the hadron thermal production, for instance, for the kaon yields and ratios [16–18]. The partial restoration of the $U_A(1)$ symmetry is closely related to the production of η meson and spin-excited hadrons in hot medium [19,20].

Effective models [21,22] are often used to describe the QCD phase structure, especially at finite baryon density, where the lattice simulation meets the fermion sign problem and cannot yet present precise results. For the study of chiral symmetry at low energy, effective models at hadron level can include only scalar and pseudoscalar mesons. In this work we choose the linear sigma model which has been widely discussed in vacuum [23]. The simplest version of this model is with the symmetry of $SU_L(2) \times SU_R(2)$ or $O(4)$, including only the Goldstone modes π and their partner, the σ meson. The linear sigma model is considered as a good laboratory for various approximation methods like mean-field and the Cornwall-Jackiw-Tomboulis (CJT) approximation. In the framework of this model, the σ and π properties have been deeply investigated in vacuum and hot medium [24–26]. The model is also extended to include quarks in the fundamental representation coupled to the mesons in Yukawa form. However, in the $SU(2)$ version the $U_A(1)$ anomaly cannot be properly studied, since there are not enough flavors for η and η' mesons which are related to the anomaly. In order to study chiral symmetry and $U_A(1)$ symmetry at the same time, the flavor symmetry group is chosen as $SU_L(3) \times SU_R(3)$ in this work.

The pion, kaon, and eta mesons are the Goldstone modes corresponding to the spontaneous $SU_A(3)$ symmetry breaking. These zero mass mesons are guaranteed by the Nambu-Goldstone theorem in vacuum as well as at low temperature $T < T_c$. However, in the mean-field approximation [24,25] and the CJT approximation [26,27], the Nambu-Goldstone theorem is destroyed at low temperature. In this work we use the functional renormalization group (FRG) method to study chiral symmetry and $U_A(1)$ symmetry in the $SU(3)$ linear sigma model at finite temperature. As a nonperturbative method [28–30], the FRG

has been used to study phase transitions in various systems like cold atom gas [31], nucleon gas [32], and hadron gas [33–38]. By solving the flow equation which connects physics at different momentum scales, the FRG shows a great power to describe the phase transitions and the corresponding critical phenomena, which are normally difficult to be controlled in the mean-field approximation because of the absence of quantum fluctuations. Instead of adding hot loops to the thermodynamic potential in the usual ways of going beyond mean field, the FRG effective potential at tree level of mean-field approximation includes already quantum fluctuations through the mass and coupling constant renormalization and can guarantee the Nambu-Goldstone theorem in chiral symmetry breaking phase.

We proceed as follows. In Sec. II, we briefly review the $SU(3)$ linear sigma model, following the notation in Ref. [27], and apply the functional renormalization to the model. The flow equations are derived, in the general case, with explicit chiral breaking terms, and the one for the chiral condensate can be solved analytically in the chiral limit. In Sec. III we present the numerical results for the light and strange quark condensates and the topological susceptibility at finite temperature. Finally, in Sec. IV we summarize our results.

II. APPLICATION OF FUNCTIONAL RENORMALIZATION TO THE $SU(3)$ LINEAR SIGMA MODEL

The $SU_L(3) \times SU_R(3)$ linear sigma model has been widely studied in mean-field and CJT approximation in vacuum and at finite temperature [27,39,40]. Following the notations in Ref. [27], the Lagrangian density of the model is expressed as

$$\begin{aligned}\mathcal{L} = {} & \mathrm{Tr}(\partial_\mu \phi^\dagger \partial^\mu \phi - m^2 \phi^\dagger \phi) + c[\mathrm{Det}(\phi) + \mathrm{Det}(\phi^\dagger)] \\ & - \lambda_1 [\mathrm{Tr}(\phi^\dagger \phi)]^2 - \lambda_2 \mathrm{Tr}(\phi^\dagger \phi)^2 + \mathrm{Tr}[H(\phi + \phi^\dagger)],\end{aligned} \tag{1}$$

where the meson matrix $\phi = T_a \phi_a$ and the trace Tr are defined in the flavor space, the meson field $\phi_a = \sigma_a + i\pi_a$ contains the scalar part σ_a, and the pseudoscalar part π_a, the 3×3 Gell-Mann matrices $T_a = \lambda_a/2$ for $a = 1, \cdots, 8$ and $T_0 = 1/\sqrt{6}$ for $a = 0$ obey the relations $\mathrm{Tr}(T_a T_b) = \delta_{ab}/2$, $[T_a, T_b] = i f_{abc} T_c$, and $\{T_a, T_b\} = d_{abc} T_c$ with the structure constants f_{abc} and d_{abc}, m^2 as the mass parameter, and c, λ_1, and λ_2 as the coupling constants.

The Lagrangian density (1) is invariant under the $SU_L(3) \times SU_R(3)$ transformation, except the last term which explicitly breaks chiral symmetry,

$$\mathrm{Tr}[H(\phi + \phi^\dagger)] = h_a \sigma_a, \tag{2}$$

where the matrix H is defined as $H = h_a T_a$ with nine parameters h_a.

The determinant term in (1) explicitly breaks the $U_A(1)$ symmetry, which in QCD is violated by the anomaly. If the coefficient c of the $U_A(1)$ anomaly term vanishes, the symmetry group of the system is enlarged to $U_L(3) \times U_R(3)$.

In vacuum and at finite temperature but zero density, there are only scalar condensates

$$\langle \phi \rangle = T_a \langle \sigma \rangle_a, \tag{3}$$

where $\langle X \rangle$ means the ensemble average of the operator X. To simplify the notation, we use $\bar{\sigma}$ to replace $\langle \sigma \rangle$ in the following. Making a shift for the meson field $\phi \to \langle \phi \rangle + \delta\phi$ and substituting it into the Lagrangian density (1), the effective potential of the system at classical level can be written as

$$\begin{aligned}U(\bar{\sigma}) = {} & \frac{m^2}{2} \bar{\sigma}_a^2 - G_{abc} \bar{\sigma}_a \bar{\sigma}_b \bar{\sigma}_c \\ & + \frac{1}{3} F_{abcd} \bar{\sigma}_a \bar{\sigma}_b \bar{\sigma}_c \bar{\sigma}_d - h_a \bar{\sigma}_a,\end{aligned} \tag{4}$$

and the dynamical masses generated by the condensates can be extracted from the coefficients of the term $(\delta\phi)^2$ and form two 9×9 matrices M_S and M_P for the scalar and pseudoscalar mesons,

$$\begin{aligned}(M_S^2)_{ab} &= m^2 \delta_{ab} - 6 G_{abc} \bar{\sigma}_c + 4 F_{abcd} \bar{\sigma}_c \bar{\sigma}_d, \\ (M_P^2)_{ab} &= m^2 \delta_{ab} + 6 G_{abc} \bar{\sigma}_c + 4 H_{abcd} \bar{\sigma}_c \bar{\sigma}_d\end{aligned} \tag{5}$$

with the coefficients defined as

$$\begin{aligned}G_{abc} = {} & \frac{c}{6}\Big[d_{abc} + \frac{9}{2} d_{000} \delta_{a0} \delta_{b0} \delta_{c0} \\ & - \frac{3}{2}(\delta_{a0} d_{0bc} + \delta_{b0} d_{a0c} + \delta_{c0} d_{ab0})\Big], \\ F_{abcd} = {} & \frac{\lambda_1}{4}(\delta_{ab}\delta_{cd} + \delta_{ad}\delta_{bc} + \delta_{ac}\delta_{bd}) \\ & + \frac{\lambda_2}{8}(d_{abe} d_{ecd} + d_{ade} d_{ebc} + d_{ace} d_{ebd}), \\ H_{abcd} = {} & \frac{\lambda_1}{4}\delta_{ab}\delta_{cd} + \frac{\lambda_2}{8}(d_{abe} d_{ecd} + f_{ade} d_{ebc} + f_{ace} d_{ebd}).\end{aligned} \tag{6}$$

The physical condensates are determined by minimizing the potential,

$$\frac{\partial U(\bar{\sigma})}{\partial \bar{\sigma}_a} = 0, \tag{7}$$

which leads to the gap equations

$$m^2 \bar{\sigma}_a - 3 G_{abc} \bar{\sigma}_b \bar{\sigma}_c + \frac{4}{3} F_{abcd} \bar{\sigma}_b \bar{\sigma}_c \bar{\sigma}_d - h_a = 0. \tag{8}$$

In different thermodynamic environments, the condensate $\langle \phi \rangle$ can be further simplified. Since the isospin zero mesons σ_0 and σ_8 or σ_η and $\sigma_{\eta'}$ can couple to the vacuum without violating Lorentz invariance and parity, the

classical field matrix $\langle\phi\rangle$ and the coefficient matrix H in the chiral breaking term contain only two components, $\langle\phi\rangle = T_0\bar{\sigma}_0 + T_8\bar{\sigma}_8$ and $H = T_0 h_0 + T_8 h_8$. In order to simplify the expressions, we make a rotation for the condensates $\bar{\sigma}_0$ and $\bar{\sigma}_8$ and the chiral breaking parameters h_0 and h_8,

$$\begin{aligned} \bar{\sigma}_u &= \sqrt{\frac{2}{3}}\bar{\sigma}_0 + \sqrt{\frac{1}{3}}\bar{\sigma}_8, \qquad \bar{\sigma}_s = \sqrt{\frac{1}{3}}\bar{\sigma}_0 - \sqrt{\frac{2}{3}}\bar{\sigma}_8, \\ h_u &= \sqrt{\frac{2}{3}}h_0 + \sqrt{\frac{1}{3}}h_8, \qquad h_s = \sqrt{\frac{1}{3}}h_0 - \sqrt{\frac{2}{3}}h_8. \end{aligned} \tag{9}$$

In terms of the rotated condensates $\bar{\sigma}_u$ and $\bar{\sigma}_s$ and the rotated breaking parameters h_u and h_s, the classical potential and the gap equations can be explicitly expressed as

$$\begin{aligned} U(\bar{\sigma}_u, \bar{\sigma}_s) = \frac{m^2}{2}(\bar{\sigma}_u^2 + \bar{\sigma}_s^2) - \frac{c}{2\sqrt{2}}\bar{\sigma}_u^2\bar{\sigma}_s + \frac{\lambda_1}{4}(\bar{\sigma}_u^2 + \bar{\sigma}_s^2)^2 \\ + \frac{\lambda_2}{8}(\bar{\sigma}_u^4 + 2\bar{\sigma}_s^4) - h_u\bar{\sigma}_u - h_s\bar{\sigma}_s \end{aligned} \tag{10}$$

and

$$\begin{aligned} m^2\bar{\sigma}_u - \frac{1}{\sqrt{2}}c\bar{\sigma}_u\bar{\sigma}_s + \lambda_1(\bar{\sigma}_u^2 + \bar{\sigma}_s^2)\bar{\sigma}_u + \frac{1}{2}\lambda_2\bar{\sigma}_u^3 = h_u, \\ m^2\bar{\sigma}_s - \frac{1}{2\sqrt{2}}c\bar{\sigma}_u^2 + \lambda_1(\bar{\sigma}_u^2 + \bar{\sigma}_s^2)\bar{\sigma}_s + \lambda_2\bar{\sigma}_s^3 = h_s. \end{aligned} \tag{11}$$

For the meson mass matrices M_S and M_P, each has only one independent off-diagonal element $M_{08}^2 = M_{80}^2$ and four independent diagonal elements M_{00}^2, M_{88}^2 and

$$\begin{aligned} m_{a_0}^2 &= (M_S^2)_{11} = (M_S^2)_{22} = (M_S^2)_{33}, \\ m_\kappa^2 &= (M_S^2)_{44} = (M_S^2)_{55} = (M_S^2)_{66} = (M_S^2)_{77}, \\ m_\pi^2 &= (M_P^2)_{11} = (M_P^2)_{22} = (M_P^2)_{33}, \\ m_K^2 &= (M_P^2)_{44} = (M_P^2)_{55} = (M_P^2)_{66} = (M_P^2)_{77}, \end{aligned} \tag{12}$$

and diagonalizing the meson subspace $a = 0, 8$ generates the pseudoscalar mesons η and η' and the corresponding scalar mesons. There are six parameters in the model, the mass m, the three coupling constants c, λ_1, and λ_2 and the two chiral breaking parameters h_u and h_s. They should be determined by the experimental data in vacuum. Firstly, the partial conservation of axial-vector current leads to a relation between the condensates and the pion and kaon decay constants f_π and f_K,

$$\bar{\sigma}_u = f_\pi, \qquad \bar{\sigma}_s = \frac{-f_\pi + 2f_K}{\sqrt{2}}, \tag{13}$$

then the gap equations (11) can be reexpressed by the Goldstone modes π and K,

$$h_u = m_\pi^2 f_\pi, \qquad h_s = \frac{-m_\pi^2 f_\pi + 5m_K^2 f_K}{\sqrt{2}}, \tag{14}$$

and the combination of the isospin zero pseudoscalar mesons η and η' determines the couplings λ_2 and c,

$$\begin{aligned} \lambda_2 &= 2\frac{\sqrt{6}\bar{\sigma}_s m_K^2 - \sqrt{2}\bar{\sigma}_0 m_\pi^2 + \bar{\sigma}_8(m_\eta^2 + m_{\eta'}^2)}{(\bar{\sigma}_u^2 + 4\bar{\sigma}_s^2)\sigma_8}, \\ c &= \frac{m_K^2 - m_\pi^2}{f_K - f_\pi} - \lambda_2(2f_K - f_\pi). \end{aligned} \tag{15}$$

Substituting the above-obtained parameters into any of the two gap equations, one can get the relation between the mass m and the coupling λ_1. By fitting a scalar meson mass, for instance m_σ, one can then separately fix the two parameters. In summary, the six parameters m, c, λ_1, λ_2, h_u, and h_s are fitted by the experimental values of m_π, m_K, f_π, f_K, and $m_\eta^2 + m_{\eta'}^2$ and one of the scalar meson masses. It is necessary to note that, in this way, one can fix a group of parameters, but the obtained condensates may not correspond to the minimum of the potential. One should check the secondary derivative of the potential, $\partial^2 U/\partial\bar{\sigma}_i\partial\bar{\sigma}_j > 0$.

We now apply the functional renormalization group to the $SU(3)$ linear sigma model. The core quantity in the framework of FRG is the averaged effective action Γ_k at a momentum scale k in Euclidean space,

$$\Gamma_k[\langle\phi\rangle] = \int d^4x[\mathrm{Tr}(Z_k\partial_\mu\langle\phi\rangle^\dagger\partial^\mu\langle\phi\rangle) + U_k(\langle\phi\rangle) + \cdots], \tag{16}$$

where Z_k is the wave function renormalization constant, $U_k(\langle\phi\rangle)$ is the classical potential (10) but with renormalized mass and coupling parameters m_k, c_k, λ_{1k}, and λ_{2k} and scale dependent condensates $\bar{\sigma}_{uk}$ and $\bar{\sigma}_{sk}$, and the symbol $\cdots$ stands for the high-order terms of the field $\langle\phi\rangle$. The scale dependence of the averaged action is characterized by the flow equation [28–30] in momentum representation,

$$\frac{\partial\Gamma_k[\langle\phi\rangle]}{\partial k} = \frac{1}{2}\int\frac{d^4p}{(2\pi)^4}\,\mathrm{Tr}\left[(\Gamma_k^{(2)}[\langle\phi\rangle] + R_k)^{-1}\frac{\partial R_k}{\partial k}\right], \tag{17}$$

where $\Gamma_k^{(2)}$ is the second-order functional derivative of the averaged action $\Gamma_k^{(2)}[\langle\phi\rangle] = \delta^2\Gamma_k/\delta\langle\phi\rangle^2$, and the infrared cutoff function R_k, which is used to suppress quantum fluctuations at low momentum $p < k$, is chosen as the optimized regulator function $R_k = (k^2 - p^2)\theta(k^2 - p^2)$ [41]. From our numerical calculation shown in the next section, the symmetry restoration and meson mass spectra at finite temperature are not sensitive to the choice of the cutoff function [42].

Following the effective action flow starting from the ultraviolet momentum $k = \Lambda$, the physics we are interested in could be obtained at $k = 0$.

By assuming the space-time independence of the classical field $\langle\phi\rangle$, the effective action to the lowest order is determined by the classical potential only,

$$\Gamma_k = \int d^4x U_k(\langle\phi\rangle). \tag{18}$$

With the known infrared cutoff function R_k, after doing the three-momentum integration for the mesons at finite temperature, the FRG flow equation can be simplified as

$$\partial_k U_k = \frac{Z_{Sk}^{-1}k^4}{6\pi^2}\left(1-\frac{\eta_{Sk}}{6}\right)T\sum_n \mathrm{Tr}D_{Sk} + \frac{Z_{Pk}^{-1}k^4}{6\pi^2}\left(1-\frac{\eta_{Pk}}{6}\right)T\sum_n \mathrm{Tr}D_{Pk}, \tag{19}$$

with the meson propagators $D_{Sk}^{-1}=Z_{Sk}^{-1}(\omega_n^2+k^2)+M_S^2$ and $D_{Pk}^{-1}=Z_{Pk}^{-1}(\omega_n^2+k^2)+M_P^2$ and the definition $\eta_k=-k\partial_k Z_k^{-1}/Z_k^{-1}$, where $\omega_n=2n\pi T$ with $n=0,1,2\cdots$ is the meson Matsubara frequency in the imaginary time formalism of finite-temperature field theory, and we have considered different renormalization constants Z_{Sk} and Z_{Pk} for the scalar and pseudoscalar fields. In order to complete the set of flow equations, we need equations for the evolution of Z_{Sk} and Z_{Pk} [30]. To the one-loop level they read

$$\begin{aligned}-\partial_k Z_{Sk}^{-1} &= \frac{Z_{Sk}^{-2}k^4}{6\pi^2}T\sum_n \mathrm{Tr}(D_{Sk}^2\Gamma_{SSS}D_{Sk}^2\Gamma_{SSS}) + \frac{Z_{Pk}^{-2}k^4}{6\pi^2}T\sum_n \mathrm{Tr}(D_{Pk}^2\Gamma_{SPP}D_{Pk}^2\Gamma_{SPP}),\\ -\partial_k Z_{Pk}^{-1} &= \frac{Z_{Sk}^{-1}Z_{Pk}^{-1}k^4}{3\pi^2}T\sum_n \mathrm{Tr}(D_{Pk}^2\Gamma_{PSP}D_{Sk}^2\Gamma_{PSP}),\end{aligned} \tag{20}$$

where $(\Gamma_{SSS})_{bc}^a=\partial^3 U_k/\partial\bar\sigma_a\partial\bar\sigma_b\partial\bar\sigma_c$, $(\Gamma_{SPP})_{bc}^a=\partial^3 U_k/\partial\bar\sigma_a\partial\bar\pi_b\partial\bar\pi_c$, and $(\Gamma_{PSP})_{bc}^a=\partial^3 U_k/\partial\bar\pi_a\partial\bar\sigma_b\partial\bar\pi_c$ are 9×9 matrices for the three-line vertexes with a fixed external meson a. In the above discussion we have assumed that the wave function renormalization constant depends only on the Lorentz transformation property of the mesons but is independent of the detailed meson types. In the following numerical calculations related to the three-line vertexes, we take the Goldstone mode $a=4$.

As we will see from the numerical calculation in the next section, the contribution from the wave function renormalization to the thermodynamics of the system is very small and can be safely neglected as a first-order approximation. In this case, by taking $Z_{Sk}=Z_{Pk}=1$, the flow equation (19) is further simplified as

$$\partial_k U_k = \frac{k^4}{6\pi^2}T\sum_n \mathrm{Tr}(D_{Sk}+D_{Pk}). \tag{21}$$

Note that the parameters h_u and h_s (or h_0 and h_8), which explicitly break chiral symmetry, are scale independent, and only the condensates $\bar\sigma_u$ and $\bar\sigma_s$ (or $\bar\sigma_0$ and $\bar\sigma_8$), which spontaneously break chiral symmetry, depend on the scale k. In the treatment of the flow equation with classical potential, the mass and coupling constant renormalization leads to four k-dependent parameters m_k, c_k, λ_{1k}, and λ_{2k} controlled by the flow equation (21), and the condensates $\bar\sigma_{uk}$ and $\bar\sigma_{sk}$ are determined by the gap equations (11).

Considering the partially degenerated diagonal elements and the simple off-diagonal structure of the mass matrices M_S and M_P, the trace Tr in (21) can be easily done, and the flow equation becomes

$$\partial_k U_k = \frac{k^4}{6\pi^2}T\sum_n[\mathrm{Tr}(\mathcal{D}_{Sk}+\mathcal{D}_{Pk})+3D_{a_0k}+4D_{\kappa k}+3D_{\pi k}+4D_{Kk}] \tag{22}$$

with two 2×2 mixed matrices

$$\mathcal{M}_S=\begin{pmatrix}(M_S^2)_{00} & (M_S^2)_{08}\\ (M_S^2)_{80} & (M_S^2)_{88}\end{pmatrix},\qquad \mathcal{M}_P=\begin{pmatrix}(M_P^2)_{00} & (M_P^2)_{08}\\ (M_P^2)_{80} & (M_P^2)_{88}\end{pmatrix} \tag{23}$$

and the corresponding propagators $\mathcal{D}_{Sk}^{-1}=\omega_n^2+k^2+\mathcal{M}_S^2$ and $\mathcal{D}_{Pk}^{-1}=\omega_n^2+k^2+\mathcal{M}_P^2$. Different from the $O(4)$ model [34], while $\mathrm{Tr}(\phi^\dagger\phi)$, $\mathrm{Tr}(\phi^\dagger\phi)^2$, and $\mathrm{Det}(\phi)+\mathrm{Det}(\phi^\dagger)$ are invariant under the $SU_L(3)\times SU_R(3)$ transformation, not all the meson masses can be expressed with the eigenvalues of these operator composites.

We now expand the potential around the minimum $\bar\sigma_{uk}$ and $\bar\sigma_{sk}$. Shifting the field $\sigma_u=\bar\sigma_{uk}+\delta\sigma_{uk}$ and $\sigma_s=\bar\sigma_{sk}+\delta\sigma_{sk}$, the derivative of the potential on the left-hand side of the flow equation could be expressed as powers of $\delta\sigma_{uk}$ and $\delta\sigma_{sk}$,

$$\begin{aligned}&\dot U_k(\bar\sigma_{uk}+\delta\sigma_{uk},\bar\sigma_{sk}+\delta\sigma_{sk})\\ &\quad=\dot U_k+\frac{\partial\dot U_k}{\partial\delta\sigma_{uk}}\delta\sigma_{uk}+\frac{\partial\dot U_k}{\partial\delta\sigma_{sk}}\delta\sigma_{sk}+\frac{1}{2}\frac{\partial^2\dot U_k}{\partial\delta\sigma_{uk}^2}\delta\sigma_{uk}^2+\frac{1}{2}\frac{\partial^2\dot U_k}{\partial\delta\sigma_{sk}^2}\delta\sigma_{sk}^2\\ &\quad\quad+\frac{1}{2}\frac{\partial^2\dot U_k}{\partial\delta\sigma_{uk}\partial\delta\sigma_{sk}}\delta\sigma_{uk}\delta\sigma_{sk}\end{aligned} \tag{24}$$

with the definition $\dot U_k=\partial_k U_k$. By comparing the coefficients of $\delta\sigma_{uk}$, $\delta\sigma_{sk}$, $\delta\sigma_{uk}^2$, $\delta\sigma_{sk}^2$, and $\delta\sigma_{uk}\delta\sigma_{sk}$ on the left- and right-hand sides of the flow equation (22), one obtains four independent differential equations for the six parameters m_k^2, c_k, λ_{1k}, λ_{2k}, $\bar\sigma_{uk}$, and $\bar\sigma_{sk}$. Together with the two gap equations, their k dependence is fully determined. Note that in deriving the four flow equations, we have used the relations $\partial_k\delta\sigma_{uk}=-\partial_k\sigma_{uk}$ and $\partial_k\delta\sigma_{sk}=-\partial_k\sigma_{sk}$.

Before numerically solving the flow equations which will be done in the next section, we first discuss the chiral limit analytically. From the relation between h_8 and $\bar\sigma_8$,

$$h_8=m_\kappa^2\bar\sigma_8, \tag{25}$$

since there is no reason for the κ meson to be massless in the chiral limit, the condensate $\bar\sigma_8$ should vanish in the case of $h_0=h_8=0$. In this limit, there remains only one gap equation for the condensate $\bar\sigma_0$,

$$m^2 - \frac{c}{\sqrt{6}}\bar{\sigma}_0 + \left(\lambda_1 + \frac{\lambda_2}{3}\right)\bar{\sigma}_0^2 = 0, \tag{26}$$

and the off-diagonal elements in the mass matrices $\mathcal{M}_{S,P}$ disappear. In the phase of spontaneous chiral symmetry breaking, there are eight pseudoscalar Goldstone modes π, K, and η, which dominate the thermodynamics of the system. From the flow equation (22), the heavy modes do not contribute much to the flow, and we can keep only the terms with the Goldstone modes. In this approximation the flow equation for the chiral condensate $\bar{\sigma}_{0k}$ is decoupled from the others,

$$\begin{aligned}\partial_k \bar{\sigma}_{0k}^2 &= \frac{8k^4}{3\pi^2} T\sum_n \frac{1}{(\omega_n^2 + k^2)^2} \\ &= \frac{2k}{3\pi^2}\left(1 + 2n_k + 2\frac{k}{T}n_k + 2\frac{k}{T}n_k^2/T\right)\end{aligned} \tag{27}$$

with the Fermi-Dirac distribution $n_k = 1/(e^{k/T} - 1)$.

It is easy to see that the right-hand side of the flow equation (27) is always positive, which leads to a monotonically increasing $\bar{\sigma}_{0k}$ with the momentum scale k at any temperature. Therefore, when we start at an ultraviolet momentum Λ, the physical condensate at $k = 0$ is guaranteed to be finite from the evolution of the flow equation. On the other hand, from the meson frequencies $\omega_n = 2n\pi T$, the condensate drops down with increasing temperature at any momentum scale k, which may lead to a phase transition of chiral symmetry restoration at a critical temperature T_c. In fact, the flow equation can be analytically integrated out with the solution

$$\bar{\sigma}_{0k}^2(T) = \bar{\sigma}_{0\Lambda}^2(T) + f(\Lambda, T) - f(k, T) \tag{28}$$

with the definition

$$\begin{aligned}f(k, T) = \frac{T^2}{3\pi^2}\Bigg[5\left(\frac{k}{T}\right)^2 + 4\left(\frac{k}{T}\right)^2 n_k \\ + 12\frac{k}{T}\ln(-n_k) - 12\mathrm{Li}_2(e^{k/T})\Bigg],\end{aligned} \tag{29}$$

where $\mathrm{Li}_2(x) = \sum_{l=1}^{\infty} x^l/l^2$ is the polylogarithm function. At very high momentum, the temperature effect on the system becomes weak, and we can reasonably take the boundary condition of the flow equation $\bar{\sigma}_{0\Lambda}(T)$ at finite temperature as the one $\bar{\sigma}_{0\Lambda}(0)$ at zero temperature. The condensate $\bar{\sigma}_{0\Lambda}(0)$ is determined by reproducing the vacuum value $\bar{\sigma}_{00}(0)$,

$$\bar{\sigma}_{0\Lambda}^2(0) = \bar{\sigma}_{00}^2(0) + f(0, 0) - f(\Lambda, 0). \tag{30}$$

The critical temperature T_c for the chiral phase transition is then determined by

$$\bar{\sigma}_{0\Lambda}^2(0) + f(\Lambda, T_c) - f(0, T_c) = 0. \tag{31}$$

In the symmetry restoration phase with $T > T_c$, the potential expansion should be around the zero condensate $\bar{\sigma}_0 = 0$. In this case, all the mesons become degenerate with mass m^2, and their contributions to the flow equation are the same. The procedure for the $SU(2)$ model is discussed in Refs. [35,38].

III. NUMERICAL RESULTS

In this section we show our numerical results for chiral symmetry and $U_A(1)$ symmetry restoration at finite temperature. In the case with explicit chiral symmetry breaking, one has to solve the coupled four flow equations, if the wave function renormalization is neglected, together with the two gap equations. The initial conditions for the four differential equations at a fixed temperature are the values of the six parameters at the ultraviolet momentum Λ, namely $m_\Lambda(T)$, $c_\Lambda(T)$, $\lambda_{1\Lambda}(T)$, $\lambda_{2\Lambda}(T)$, $\bar{\sigma}_{u\Lambda}(T)$, and $\bar{\sigma}_{s\Lambda}(T)$. Considering the fact that the system at high-enough momentum is dominated by the dynamics and not affected remarkably by the temperature, the temperature dependence of the parameters at the ultraviolet momentum can be safely neglected. Therefore, we take the temperature-independent initial values $m_\Lambda(T) = m_\Lambda(0)$, $c_\Lambda(T) = c_\Lambda(0)$, $\lambda_{1\Lambda}(T) = \lambda_{1\Lambda}(0)$, $\lambda_{2\Lambda}(T) = \lambda_{2\Lambda}(0)$, $\bar{\sigma}_{u\Lambda}(T) = \bar{\sigma}_{u\Lambda}(0)$, and $\bar{\sigma}_{s\Lambda}(T) = \bar{\sigma}_{s\Lambda}(0)$, and they are so chosen to reproduce their vacuum values at $k = 0$, discussed in Sec. II, by solving the flow equations and gap equations at zero temperature.

Figure 1 shows the evolution of the condensates $\bar{\sigma}_{uk}$, $\bar{\sigma}_{sk}$, and $\bar{\sigma}_{8k}$ at zero temperature. With increasing momentum scale k, the condensate $\bar{\sigma}_{8k}$ drops down fast and becomes only 30% of its vacuum value at $k \sim 1$ GeV. From the relation $h_8 = m_{\kappa k}^2 \bar{\sigma}_{8k}$, the k independence of the chiral breaking parameter h_8 leads to a large meson mass $m_{\kappa k}$ at $k \sim 1$ GeV. Therefore, we take 1 GeV as the ultraviolet momentum Λ for the evolution of the renormalization parameters. We have checked that the numerical results are insensitive to the value of the momentum cut Λ. Both the light and strange quark condensates $\bar{\sigma}_{uk}$ and $\bar{\sigma}_{sk}$ go up with increasing scale k, as we analyzed in the end of Sec. II, in the chiral limit.

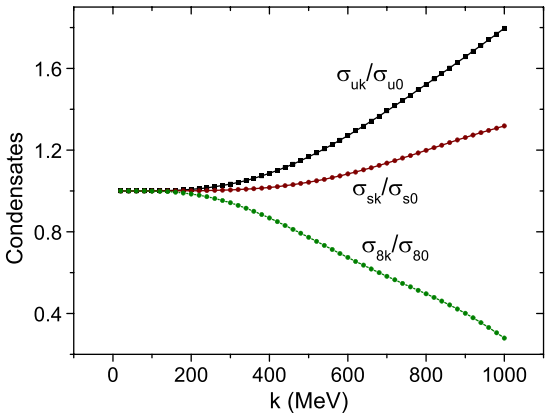

FIG. 1 (color online). The evolution of the condensates $\bar{\sigma}_{uk}$, $\bar{\sigma}_{sk}$, and $\bar{\sigma}_{8k}$ at $T = 0$, scaled by their vacuum values at $k = 0$.

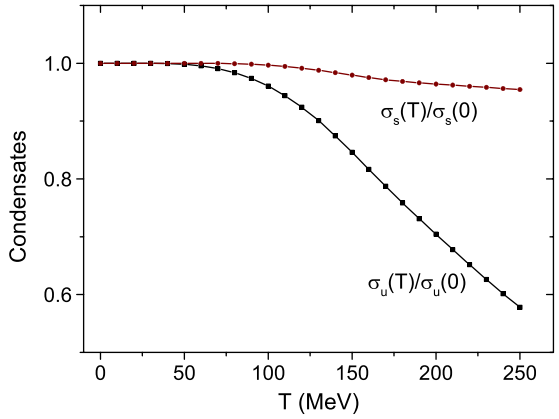

FIG. 2 (color online). The temperature dependence of the light and strange quark condensates $\bar{\sigma}_{u0}$, $\bar{\sigma}_{s0}$, scaled by their vacuum values at $T = 0$.

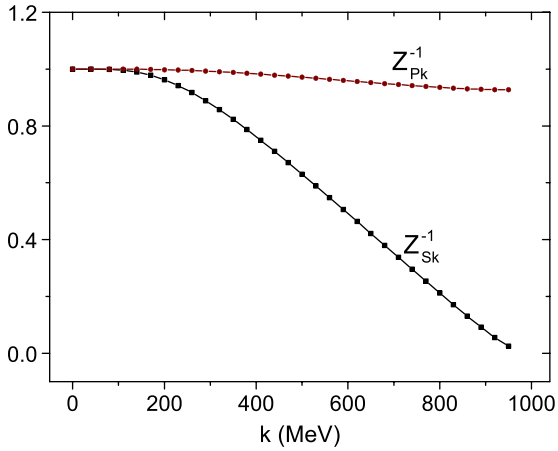

FIG. 3 (color online). The momentum scale dependence of the wave function renormalization constants at zero temperature.

The temperature dependence of the light and strange quark condensates at $k = 0$ is shown in Fig. 2. While both condensates are almost constants at low temperature $T < 50$ MeV, they monotonically decrease at high-enough temperature, as we expected from the analysis in the chiral limit. Since strange quarks are much heavier than light quarks, which is reflected in the values of the explicit symmetry breaking parameters h_u and h_s, the $SU(2)$ symmetry restoration should be much faster than the $SU(3)$ symmetry restoration. This is the reason why the light quark condensate drops more rapidly than the strange quark condensate. The qualitative behavior of the condensates shown here is similar to what is obtained in the framework of mean-field and CJT approximation [25,27].

What is the effect of the wave function renormalization on the condensates? Solving the flow equations (24) for the renormalized mass and coupling constants m_k^2, c_k, λ_{1k}, and λ_{2k} and (20) for the renormalized wave functions Z_{Sk} and Z_{Pk} and the gap equations (11) for the condensates $\bar{\sigma}_{uk}$ and $\bar{\sigma}_{sk}$, and taking the vacuum values $Z_{S0} = Z_{P0} = 1$ at $T = k = 0$, the momentum scale dependence of Z_{Sk}^{-1} and Z_{Pk}^{-1} at zero temperature is shown in Fig. 3. While the scalar part varies strongly with the scale k, the renormalization for the pseudoscalar mesons, among which the Goldstone modes dominate the thermodynamics of the system, is a very smooth function in the whole region $0 < k < \Lambda$. Considering the fact of $\eta_k \propto \partial_k Z_k^{-1}$ in the flow equation (19), the contribution from the wave function renormalization to the averaged action is expected to be slight. From Fig. 4, the temperature dependence of the light and strange quark condensates, including the contribution from the wave function renormalization, is almost the same as the one shown in Fig. 2. Therefore, for the following numerical calculations, we will omit the wave function renormalization as a first-order approximation.

The $U_A(1)$ anomaly is described by the topological susceptibility [10]

$$\chi = \int d^4x \langle 0|T(Q(x)Q(0))|0\rangle \tag{32}$$

with $Q(x)$ being the topological charge determined by the QCD coupling constant g and the gauge field tensor $F_{\mu\nu}^a$,

$$Q(x) = \frac{g^2}{64\pi^2}\epsilon^{\mu\nu\rho\sigma}F_{\mu\nu}^a(x)F_{\rho\sigma}^a(x), \tag{33}$$

where $\epsilon_{\mu\nu\rho\sigma}$ is the antisymmetric tensor. By introducing the anomaly, the ninth Goldstone mode η' is no longer massless. The topological susceptibility can be related to the pseudoscalar meson masses in the linear sigma model by the Witten-Veneziano relation [3,4],

$$\chi = \frac{f_\pi^2}{6}(m_\eta^2 + m_{\eta'}^2 - 2m_K^2) = \frac{\sigma_u^2}{12}(\sqrt{6}c\sigma_0 - 3\lambda_2\sigma_8^2). \tag{34}$$

It is determined not only by the three-line coupling c but also by the four-line coupling λ_2, although the $U_A(1)$

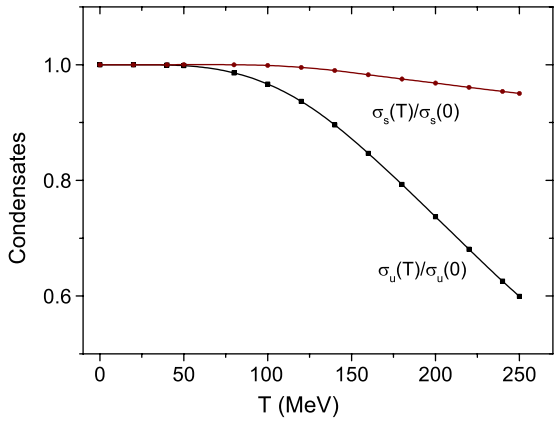

FIG. 4 (color online). The temperature dependence of the light and strange quark condensates, including the wave function renormalization.

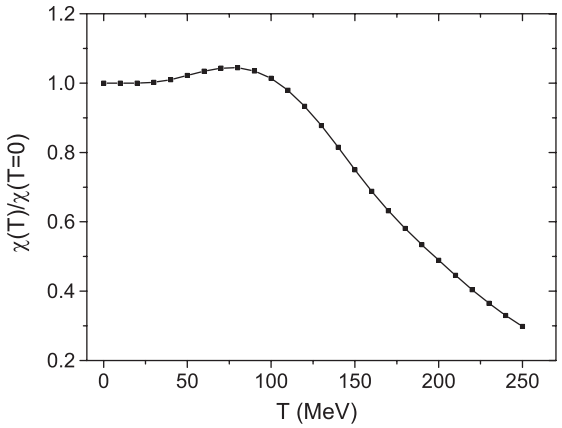

FIG. 5. The temperature dependence of the topological susceptibility χ, scaled by its vacuum value at $T = 0$.

symmetry is broken only by the determinant term which is irrelevant to λ_2.

The temperature dependence of the topological susceptibility is shown in Fig. 5. It decreases with temperature in the region of $T \geq 100$ MeV, indicating a continuous restoration of $U_A(1)$ symmetry. Different from the lattice simulation for the $SU(3)$ Yang-Mills theory [10], where the susceptibility drops down rapidly, the susceptibility remains still 30% of its vacuum value at high temperature $T = 250$ MeV. Unlike the condensates that never increase with temperature, the susceptibility shows a slight increase in the low-temperature region of $T < 100$ MeV, which is observed also in simulations in the interacting instanton liquid model [12].

Chiral symmetry and $U_A(1)$ symmetry restoration shown above control the meson masses in hot medium. The temperature dependence of the meson masses is shown in Figs. 6 and 7. There are four different mesons for each species, the triplet a_0, quartet κ, and the mixed σ and f_0 for the scalar mesons, and the triplet π, quartet K, and the mixed η and η' for the pseudoscalar mesons. As temperature increases, the scalar meson masses m_{f_0}, m_κ, and m_{a_0}

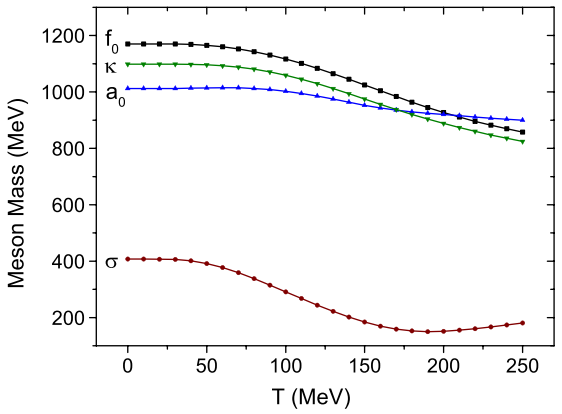

FIG. 6 (color online). The temperature dependence of the scalar meson masses.

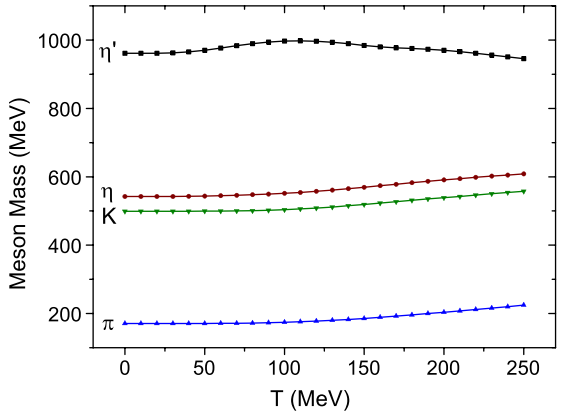

FIG. 7 (color online). The temperature dependence of the pseudoscalar meson masses.

drop down monotonically, but f_0 and κ are heavier than a_0 at $T < 200$ MeV and become lighter than a_0 at $T > 200$ MeV. The Goldstone modes π and their chiral partner σ become degenerate at high temperature, due to chiral symmetry restoration. A similar behavior is seen for the mesons a_0 and η'. At $T = 250$ MeV, there are $m_\pi \simeq m_\sigma \simeq 200$ MeV and $m_{a_0} \simeq m_{\eta'} \simeq 900$ MeV. The mixed mode η behaves similarly to the other seven Goldstone modes π and K. While the mass of the other mixed meson η' slightly goes up at low temperature and drops down at high temperature, the difference between η and η' decreases with increasing temperature, due to the partial restoration of the $U_A(1)$ symmetry.

The main difference between the FRG and the mean-field [25] and CJT [27] approximations is that the quantum fluctuations included in the FRG slow down the chiral symmetry and $U_A(1)$ symmetry restoration. The light quark condensate drops down fast around $T \sim 150$ MeV and approaches zero at $T \sim 300$ MeV in the CJT [27] but still keeps 60% of its vacuum value at $T \sim 250$ MeV in the FRG, see Fig. 2. The fast symmetry restoration makes the mesons become degenerate at high temperature [27], and the slow restoration leads to a still remarkable separation of meson masses, see Figs. 6 and 7. In Fig. 8, we showed the K and η meson masses calculated in the FRG and CJT. The two kinds of mesons become almost degenerate at $T \sim 250$ MeV in the CJT but still separate from each other at this temperature in the FRG. Note that one needs a scalar meson mass to fix the model parameters. In our calculation we took $m_\sigma = 400$ MeV [25], and it was taken as 600 MeV in the CJT [27]. While this difference changes the f_0 meson mass, the κ and a_0 in the vacuum are the same in the two approaches, since they are decoupled from σ in the model.

In the chiral limit, the condensate $\bar{\sigma}_8$ disappears and the flow equation for the condensate $\bar{\sigma}_0$ is decoupled from the others and can be analytically solved as in (28). The evolutions of $\bar{\sigma}_{0k}$ at different temperature are shown in Fig. 9. While the temperature dependence at low

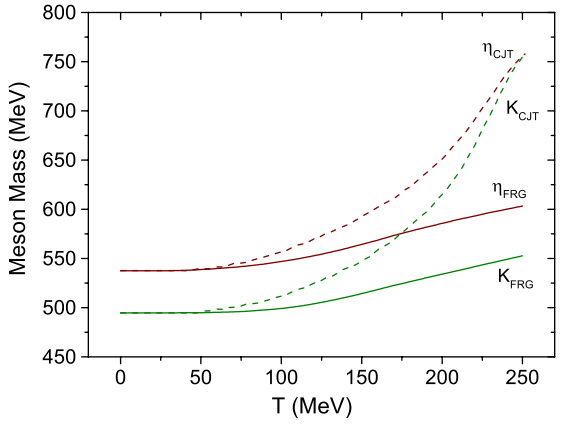

FIG. 8 (color online). The comparison of K and η meson masses between the FRG (solid lines) and CJT [27] (dashed lines) calculations.

momentum scale k is remarkable, the condensate is almost T independent when the scale is large enough. This supports our choice of T-independent initial condition at $k = \Lambda$. With increasing temperature, the solution at $k = 0$ approaches zero continuously, indicating the phase transition of chiral symmetry restoration. The temperature dependence of the physical condensate and topological susceptibility at $k = 0$ is shown in Fig. 10. The condensate drops down much faster than that in the general case with explicit chiral symmetry breaking, see Fig. 2. The critical temperature for the chiral phase transition determined by $\bar{\sigma}_{00}(T_c) = 0$ is $T_c = 130$ MeV.

The topological susceptibility (34) for the $U_A(1)$ anomaly is simplified as

$$\chi = \frac{1}{3\sqrt{6}} c\sigma_0^3 \tag{35}$$

in the chiral limit. After a rapid decrease in the vicinity of vacuum, it becomes very smooth and finally vanishes at the same critical temperature for the $SU_A(3)$ symmetry restoration.

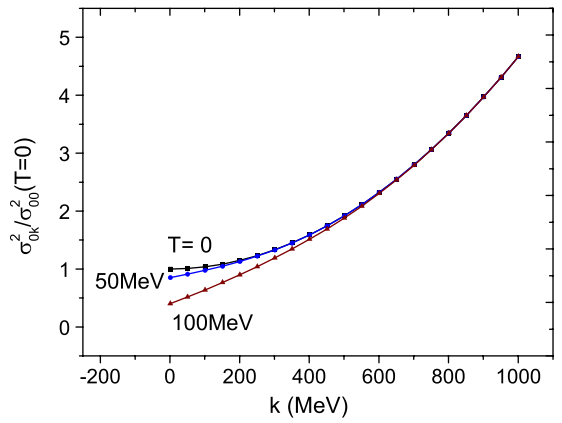

FIG. 9 (color online). The evolutions of the condensate $\bar{\sigma}_{0k}$ at different temperature in the chiral limit.

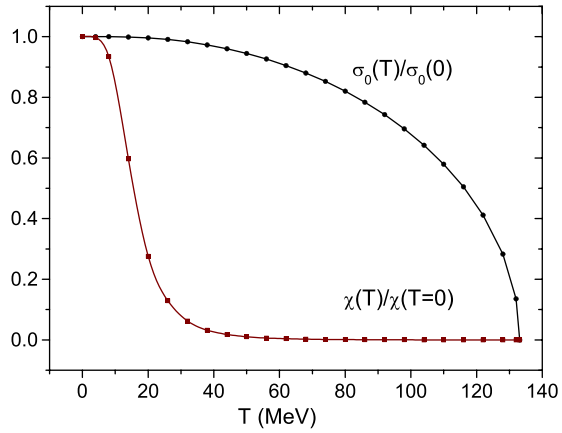

FIG. 10 (color online). The temperature dependence of the chiral condensate $\bar{\sigma}_0$ and topological susceptibility χ in chiral limit, scaled by their vacuum values.

IV. CONCLUSION

We investigated in this paper chiral symmetry and $U_A(1)$ symmetry restoration at finite temperature by applying the functional renormalization group to the $SU(3)$ linear sigma model. We derived the flow equations for the mass, coupling, and wave function renormalization parameters in the local potential approximation and the two gap equations for the light and strange quark condensates.

In the chiral limit, we analytically solved the decoupled flow equation for the chiral condensate and analyzed its momentum scale and temperature dependence. The eight Goldstone modes are guaranteed in vacuum and at finite temperature before the chiral restoration, and the two phase transitions for chiral symmetry and $U_A(1)$ symmetry restoration take place at the same critical temperature $T_c = 130$ MeV.

In the general case with explicit chiral symmetry breaking, we numerically solved the coupled flow and gap equations at finite temperature, starting from the classical potential at the ultraviolet momentum $k = \Lambda \sim 1$ GeV and extracting physics including quantum fluctuations at $k = 0$. In this case, a partial restoration of the $SU_A(3)$ and $U_A(1)$ symmetries is observed. Different from the results obtained in other approximations, like the CJT method, the light and strange quark condensates drop down with temperature slowly. As a result of the partial restoration of the two symmetries, the pseudoscalar triplet π and its chiral partner σ (the scalar triplet a_0 and η') become degenerate at high temperature, and the difference between the mixed modes η and η' gradually disappears in the limit of high temperature.

ACKNOWLEDGMENTS

The work is supported by the NSFC (Grants No. 10975084 and No. 11079024), RFDP (Grant No. 20100002110080), and MOST (Grant No. 2013CB922000).

[1] G. 't Hooft, Phys. Rev. D **14**, 3432 (1976); **18**, 2199(E) (1978).
[2] H. Leutwyler and A. V. Smilga, Phys. Rev. D **46**, 5607 (1992).
[3] E. Witten, Nucl. Phys. **B156**, 269 (1979).
[4] G. Veneziano, Nucl. Phys. **B159**, 213 (1979).
[5] C. Rosenzweig, J. Schechter, and C. G. Trahern, Phys. Rev. D **21**, 3388 (1980).
[6] R. Alkofer, Proc. Sci. FACESQCD (2010) 030 [arXiv:1102.3166].
[7] K. Kawarabayashi and N. Ohta, Nucl. Phys. **B175**, 477 (1980).
[8] K. Kawarabayashi and N. Ohta, Prog. Theor. Phys. **66**, 1789 (1981).
[9] T. Schafer, Phys. Lett. B **389**, 445 (1996).
[10] B. Alles, M. D'Elia, and A. Di Giacomo, Nucl. Phys. **B494**, 281 (1997); **B679**, 397(E) (2004).
[11] B. Alles, M. D'Elia, A. Di Giacomo, and P. W. Stephenson, Nucl. Phys. B, Proc. Suppl. **73**, 518 (1999).
[12] O. Wantz and E. P. S. Shellard, Nucl. Phys. **B829**, 110 (2010).
[13] T. Csorgo, R. Vertesi, and J. Sziklai, Phys. Rev. Lett. **105**, 182301 (2010).
[14] S. Benic, D. Horvatic, D. Kekez, and D. Klabucar, Phys. Rev. D **84**, 016006 (2011).
[15] Y. Kwon, S. H. Lee, K. Morita, and G. Wolf, Phys. Rev. D **86**, 034014 (2012).
[16] C. M. Ko, Z. G. Wu, L. H. Xia, and G. E. Brown, Phys. Rev. Lett. **66**, 2577 (1991); **67**, 1811(E) (1991).
[17] G. Q. Li and G. E. Brown, Phys. Rev. C **58**, 1698 (1998).
[18] K. Paech, A. Dumitru, J. Schaffner-Bielich, H. Stoecker, G. Zeeb, D. Zschiesche, and S. Schramm, Acta Phys. Hung. A **21**, 151 (2004).
[19] Z. Huang and X. N. Wang, Phys. Rev. D **53**, 5034 (1996).
[20] B. Keren-Zur and Y. Oz, J. High Energy Phys. 06 (2010) 006.
[21] G. Amelino-Camelia, Phys. Lett. B **407**, 268 (1997).
[22] J. Schaffner-Bielich, Phys. Rev. Lett. **84**, 3261 (2000).
[23] S. Gasiorowicz and D. A. Geffen, Rev. Mod. Phys. **41**, 531 (1969).
[24] N. Bilic and H. Nikolic, Eur. Phys. J. C **6**, 515 (1999).
[25] B.-J. Schaefer and M. Wagner, Phys. Rev. D **79**, 014018 (2009).
[26] H. Mao, N. Petropoulos, and W. Q. Zhao, J. Phys. G **32**, 2187 (2006).
[27] J. T. Lenaghan, D. H. Rischke, and J. Schaffner-Bielich, Phys. Rev. D **62**, 085008 (2000).
[28] J. Berges, arXiv:hep-ph/9902419.
[29] H. Gies, arXiv:hep-ph/0611146.
[30] P. Kopietz, L. Bartosch, and F. Schutz, Lect. Notes Phys. **798**, 1 (2010).
[31] S. Floerchinger, R. Schmidt, S. Moroz, and C. Wetterich, Phys. Rev. A **79**, 013603 (2009).
[32] B. Friman, K. Hebeler, and A. Schwenk, Lect. Notes Phys. **852**, 245 (2012).
[33] T. K. Herbst, J. M. Pawlowski, and B. J. Schaefer, Phys. Lett. B **696**, 58 (2011).
[34] B. Stokic, B. Friman, and K. Redlich, Eur. Phys. J. C **67**, 425 (2010).
[35] O. Bohr, B. J. Schaefer, and J. Wambach, Int. J. Mod. Phys. A **16**, 3823 (2001).
[36] J. P. Blaizot, A. Ipp, R. Mendez-Galain, and N. Wschebor, Nucl. Phys. **A784**, 376 (2007).
[37] B. J. Schaefer and H. J. Pirner, Nucl. Phys. **A660**, 439 (1999).
[38] K. Fukushima, K. Kamikado, and B. Klein, Phys. Rev. D **83**, 116005 (2011).
[39] R. D. Pisarski and F. Wilczek, Phys. Rev. D **29**, 338 (1984).
[40] L. H. Chan and R. W. Haymaker, Phys. Rev. D **7**, 402 (1973).
[41] D. F. Litim, Phys. Rev. D **64**, 105007 (2001).
[42] G. Papp, B. J. Schaefer, H. J. Pirner, and J. Wambach, Phys. Rev. D **61**, 096002 (2000).